



IL-33 targeting attenuates intestinal mucositis and enhances effective tumor chemotherapy in mice

Rodrigo Guabiraba, Anne-Gaëlle Besnard, Gustavo Batista Menezes, Thomas Secher, M. S. Jabir, S. S. Amaral, Harald Braun, Roberto C.P. Lima-Junior, R. A. Ribeiro, Fernando de Queiroz Cunha, et al.

► To cite this version:

Rodrigo Guabiraba, Anne-Gaëlle Besnard, Gustavo Batista Menezes, Thomas Secher, M. S. Jabir, et al.. IL-33 targeting attenuates intestinal mucositis and enhances effective tumor chemotherapy in mice. *Mucosal Immunology*, 2014, 7 (5), pp.1079-1093. 10.1038/mi.2013.124 . hal-02633989

HAL Id: hal-02633989

<https://hal.inrae.fr/hal-02633989>

Submitted on 23 Feb 2024

HAL is a multi-disciplinary open access archive for the deposit and dissemination of scientific research documents, whether they are published or not. The documents may come from teaching and research institutions in France or abroad, or from public or private research centers.

L'archive ouverte pluridisciplinaire **HAL**, est destinée au dépôt et à la diffusion de documents scientifiques de niveau recherche, publiés ou non, émanant des établissements d'enseignement et de recherche français ou étrangers, des laboratoires publics ou privés.

Published in final edited form as:

Mucosal Immunol. 2014 September ; 7(5): 1079–1093. doi:10.1038/mi.2013.124.

IL-33 targeting attenuates intestinal mucositis and enhances effective tumour chemotherapy in mice

R Guabiraba¹, A G Besnard¹, G B Menezes², T Secher³, M S Jabir^{1,9}, S S Amaral², H Braun^{5,6}, R C P Lima-Junior⁷, R A Ribeiro⁷, F Q Cunha⁸, G J Graham¹, M M Teixeira⁴, R Beyaert^{5,6}, and F Y Liew^{1,10}

¹Institute of Infection, Immunity and Inflammation, Glasgow Biomedical Research Centre, University of Glasgow, UK.

²Immunobiophotonics, Department of Morphology, Biological Sciences Institute, Federal University of Minas Gerais, Brazil.

³Centre de Physiopathologie de Toulouse Purpan, U1043, Institut National de la Santé et de la Recherche Médicale, Toulouse, France.

⁴Immunopharmacology, Department of Biochemistry and Immunology, Biological Sciences Institute, Federal University of Minas Gerais, Brazil.

⁵Department of Biomedical Molecular Biology, Ghent University, Ghent, Belgium.

⁶VIB Inflammation Research Center, Ghent, Belgium.

⁷Department of Physiology and Pharmacology, Faculty of Medicine, Federal University of Ceará, Brazil.

⁸Department of Pharmacology, School of Medicine of Ribeirão Preto (FMRP), University of São Paulo, Brazil.

⁹Department of Biotechnology, University of Technology, Baghdad, Iraq.

¹⁰CEGMR, King Abdulaziz University, Jeddah, Saudi Arabia.

Abstract

Intestinal damage and severe diarrhea are serious side effects of cancer chemotherapy and constrain the usage of most such therapies. Here we show that IL-33 mediates the severe intestinal mucositis in mice treated with Irinotecan (CPT-11), a commonly used cancer chemotherapeutic agent. Systemic CPT-11 administration led to severe mucosal damage, diarrhea and body weight loss concomitant with the induction of IL-33 in the small intestine (SI). This mucositis was markedly reduced in mice deficient in the IL-33R (ST2^{-/-}). Moreover, recombinant IL-33 exacerbated the CPT-11-induced mucositis, whereas IL-33 blockade with anti-IL-33 antibody or soluble ST2 markedly attenuated the disease. CPT-11-treatment increased neutrophil

Corresponding authors: Foo Y. Liew or Rodrigo Guabiraba, Institute of Infection, Immunity and Inflammation, Glasgow Biomedical Research Centre, University of Glasgow, 120 University Place, Glasgow, G12 8TA, UK. Tel: +44 (0)1413308408. foo.liew@glasgow.ac.uk or rguabiraba@gmail.com.

SUPPLEMENTARY MATERIAL is linked to the online version of the paper at <http://www.nature.com/mi>.

DISCLOSURE The authors declared no conflict of interest.

accumulation in the SI and adhesion to mesenteric veins. Supernatants from SI explants treated with CPT-11 enhanced transmigration of neutrophils in vitro in an IL-33, CXCL1/2 and CXCR2-dependent manner. Importantly, IL-33 blockade reduced mucositis and enabled prolonged CPT-11 treatment of ectopic CT26 colon carcinoma leading to a beneficial outcome of the chemotherapy. These results suggest that inhibition of the IL-33/ST2 pathway may represent a novel approach to limit mucositis and thus improve the effectiveness of chemotherapy.

INTRODUCTION

Mucositis is defined by inflammatory and ulcerative lesions of the oral and gastrointestinal mucosa commonly associated with cancer chemotherapy^{1, 2}. Combination therapy such as radiation with concurrent chemotherapy may further increase the severity of mucositis that often leads to dosage reduction or premature cessation of cancer treatment^{3, 4}. Thus, reagents that can attenuate chemotherapy-induced mucositis would be highly beneficial in enabling prolonged therapy and hence more effective cancer treatment.

Mucositis develops as a consequence of epithelial injury². However, its pathophysiology is complex and involves multiple steps¹ including the generation of reactive oxygen species (ROS) and reactive nitrogen species, together leading to epithelial damages⁵. Chemotherapy directly causes DNA damage and cell death⁶ with activation of NFκB and up-regulation of cytokine production⁷⁻¹⁰. In the ulcerative phase, epithelial erosion can lead to risk of microbial infiltration and septic shock¹¹.

CPT-11, a topoisomerase I inhibitor, is an anti-proliferative drug used to treat different types of human malignancies, such as metastatic colorectal cancer^{3, 4}. CPT-11 is metabolized in the liver and converted to SN-38, the active metabolite, by carboxylesterases (CES)-mediated hydrolysis³. The intestinal microbiota enzymatic system is also involved in the metabolism of CPT-11, and the compound can be metabolized in different in vitro and ex vivo experimental settings^{3, 12-14}. The clinical pharmacokinetic properties of CPT-11 and its metabolites appears to be crucial for optimal anticancer chemotherapy³.

IL-33 is a member of the IL-1 cytokine family, which includes also IL-1 and IL-18 (ref. 15). IL-33 is crucial for the induction of Type 2 immune responses by promoting the synthesis of cytokines such as IL-5 and IL-13 by Th2 lymphocytes, mast cells, basophils and eosinophils. IL-33 is also involved in the induction of non-Th2-type acute and chronic inflammation as a pro-inflammatory cytokine^{15, 16}. IL-33 signals via a heteromeric receptor that consists of ST2 and IL-1R accessory protein¹⁷. ST2 (also known as T1), the transmembrane protein encoded by the *ST2* gene, is expressed especially on immune cells such as mast cells and activated Th2 cells^{18, 19}. The *ST2* gene is alternatively spliced to produce a soluble form (sST2), which acts as an IL-33 decoy receptor²⁰. IL-33 is produced as a precursor protein (pro-IL-33) that is proteolytically converted to mature IL-33. Both forms are released by necrotic cells and have biological activity¹⁹⁻²¹. Thus IL-33 released by necrotic cells during tissue injury may play a DAMP/alarmin-like role in the induction of inflammation¹⁶.

IL-33 is expressed by the gut epithelial cells¹⁵, but current data on the role of IL-33 in the onset of inflammatory bowel diseases (IBD) is controversial²². IL-33 appears to enhance intestinal inflammation in disease models driven by Th2 and innate immune responses, such as in senescence-accelerated-prone mice (SAMP) and experimental acute colitis, and possibly in ulcerative colitis (UC) patients²³⁻²⁷. Up-regulation of IL-33 in patients with IBD has been demonstrated by several reports (reviewed in ref. 23). However, the participation of IL-33 in patients undergoing chemotherapy treatment has so far not been documented. High levels of IL-33 during acute inflammation are likely to exacerbate tissue damage, whereas they may enhance tissue repair during recovery^{22, 26}. Thus, the initial features of the specific immune response and the timing of IL-33 blockade may define the disease outcome.

Animal models of CPT-11-induced mucositis are used extensively to identify the key players in disease pathogenesis, such as cytokines and chemokines^{10, 12, 28-30}. However, the sequence of events following mucosal damage induced by chemotherapy remains undefined. Here we report a hitherto unrecognized mechanism by which IL-33 mediates CPT-11-induced mucositis via the attraction of neutrophils to the site of inflammation and tissue damage in the small intestine. Targeting the IL-33/ST2 pathway confers protection and tissue preservation. In a murine model of CT26 ectopic colon carcinoma, IL-33 blockade enables prolonged and effective chemotherapy, resulting in markedly reduced tumour growth. These results suggest that the IL-33/ST2 pathway might be a novel therapeutic target for an enhanced beneficial outcome of cancer chemotherapy.

RESULTS

IL-33 is produced in chemotherapy-induced mucositis in the small intestine

Several pro-inflammatory cytokines have been associated with the severity of chemotherapy-induced mucositis, although their role in disease pathogenesis is not fully understood^{1, 2, 10, 31}. To investigate the role of IL-33 in the inflammatory response induced by CPT-11 (Irinotecan) chemotherapy, BALB/c mice were injected intraperitoneally (i.p.) for 4 consecutive days (0 to 3) with CPT-11 and mucositis was analyzed on day 4. The production of IL-33 and its soluble receptor sST2 was significantly elevated in the small intestine (SI) compared to that of the PBS-treated control mice (Figure 1a). The production of IL-33 and sST2 appears to be confined to the mucosal compartment since they were not detected in the serum (data not shown). We then verified this observation using SI explant of naïve mouse in vitro. CPT-11 stimulated IL-33 production by the SI explant in a dose-dependent manner (Figure 1b). Furthermore, SN-38, the active metabolite of CPT-11, also induced IL-33 synthesis by the SI explant in vitro (Figure 1b).

To investigate the cellular source of IL-33, the SI of CPT-11 treated mice was analyzed by IHC staining. IL-33⁺ cells were markedly increased in the epithelial cells of the villi and the crypts of the CPT-11-treated mice compared to that of the PBS-treated mice (Figure 1c). Positive staining for IL-33 was seen in the whole epithelia, suggesting that both putative stem cells/proliferating progenitor cells (crypts) and differentiated cells (villi, including goblet cells, enterocytes and entero-endocrine cells) could release IL-33. IHC staining using Annexin V, which binds to phosphatidylserine to identify apoptotic cells, confirmed that

both differentiated and proliferating epithelial cells were damaged by CPT-11 and are potential sources of IL-33 (Figure 1c). To confirm this observation, we then isolated the epithelial cells (CD45⁻ cytokeratin⁺) from the SI of naïve mice and cultured the cells for 6 h with CPT-11 in vitro and analyzed the expression of IL-33 by FACS. CPT-11 stimulated epithelial cells produce IL-33 in a concentration-dependent manner (Figure 1d,e).

We then examined the relevance of our observation in human cells using the epithelial-like human colon carcinoma Caco-2 cells. Caco-2 cells produced significant amounts of IL-33 when cultured in vitro with CPT-11 and SN-38 (Figure 1f). There was also a modest but significant reduction in cell viability of Caco-2 cells at this time point (10% for CPT-11 and 15% for SN-38 as compared to control group). Together these results demonstrate that CPT-11 effectively induces IL-33 production by the epithelial cells of the SI.

IL-33 is associated with the pathogenesis of chemotherapy-induced mucositis

We next investigated the role of the IL-33/ST2 pathway in the pathogenesis of mucositis. We treated wild-type BALB/c mice and ST2^{-/-} mice (BALB/c background) with CPT-11 with or without recombinant murine IL-33. WT mice treated with CPT-11 showed significant body weight loss (~10%) by day 3 and diarrhea (clinical score 1-2) on day 4 (Figure 2a,b). These clinical changes were accompanied by severe systemic leucopenia, shortened villi and increased plasma leakage in the SI (Figure 2c-e). All these parameters were significantly exacerbated by the additional daily treatment with exogenous IL-33 (200 ng/mouse). ST2^{-/-} mice did not respond to recombinant murine IL-33 treatment in any of the clinical parameters evaluated (Figure 2a,b). Furthermore, ST2^{-/-} mice developed significantly attenuated disease with reduced weight loss, clinical score (clinical score 0-1), leucopenia, plasma leakage; but increased SI villi length, as compared to the PBS control group (Figure 2a-e). Histopathological analysis of the SI of WT mice revealed a dramatic remodeling of the small intestinal mucosa, with different degrees of submucosal edema, submucosal hemorrhage, venous congestion, inflammatory submucosal leukocyte infiltrate, shortening of villi and reduction in goblet cell numbers as assessed by H&E and PAS staining (Figure 2f-i). Mice treated with CPT-11 + IL-33 showed even more severe outcome in all these parameters and presented increased signs of hemorrhage, venous congestion and villi reduction. A modest but significant deleterious effect of CPT-11 + IL-33 treatment in the mucosa starts to appear on day 3 in the WT mice (data not shown). In contrast, ST2^{-/-} mice presented a preserved intestinal architecture, with subtle leukocyte infiltrate and discrete villi shortening. Villi atrophy and crypt destruction are the main causes of diarrhea in mice³²⁻³⁴

Since mucosal damage due to chemotherapy has been associated with increased blood bacteremia^{11, 32, 35}, we also measured the level of bacteremia by qPCR. Mice treated with CPT-11 developed markedly increased bacteremia which was significantly elevated by the co-treatment with IL-33 (clinical score 2-3), while ST2^{-/-} mice treated with CPT-11 (clinical score 0-1) had significantly less bacteremia compared to that of the WT mice (Figure 2j). Together these results demonstrate that CPT-11-induced mucositis is dependent on the IL-33/ST2 pathway.

The role of chemokines in the CPT-11-induced mucositis

The histopathological changes observed above were associated with a significant increase in the level of expression of the apoptosis markers Caspase 9, Caspase 3 and PARP (cleaved forms); and Bax in the SI (Supplementary Figure S1a-c online). IL-33 further increased the expression of these apoptotic markers, which were significantly reduced in ST2^{-/-} mice. We also investigated the production of selected chemokines in the serum (Supplementary Figure S1d-f online) and in the SI (Supplementary Figure S1g-i online). The concentrations of CXCL1/KC, CXCL2/MIP-2 and CCL2/JE in the serum were all elevated in the CPT-11-treated mice compared to untreated mice. All these chemokines were further increased by the additional treatment with IL-33. In contrast, the levels of these chemokines remained at the control (PBS) level in the ST2^{-/-} mice. Importantly, IL-33 treatment increased the level of IL-33 in the SI induced by CPT-11. This increase was not due to the injected rmIL-33, since the level of IL-33 in IL-33-treated WT mice not given CPT-11 remained low. Moreover, the SI was perfused prior to cytokine/chemokine assays (see Methods). ST2^{-/-} mice treated with CPT-11 had significantly lower concentration of IL-33 in the SI compared CPT-11-treated WT mice (Supplementary Figure 1j online). These data suggest that IL-33-mediated chemokine induction may be an important, though not the only, mechanism involved in CPT-11-induced mucositis. In addition, IL-33 released by damaged epithelial cells (i.e. IL-33⁺ Annexin V⁺ cells) could increase its own synthesis by activating the ST2 receptor in an autocrine manner³⁶. It has been shown that the local allergic inflammatory response are amplified by DC-produced IL-33 through potential autocrine regulation³⁷. In line with this observation, the ST2 receptor is known to be widely expressed in intestinal epithelial cells²⁵.

Neutrophils play a key role in CPT-11/IL-33-induced intestinal mucositis

The marked increase of CXCL1 and CXCL2 during mucositis induced by the CPT-11/IL-33/ST2 pathway suggests that neutrophils might play an important role in the downstream events leading to mucosal damage. Although neutropenia and neutropenic fever are frequently reported in patients undergoing chemotherapy, the role of neutrophils in the context of CPT-11/IL-33-induced inflammatory response is unclear³⁸. Studies in rodents suggested that neutrophils may accumulate in the intestinal mucosa after chemotherapeutic treatment^{9, 10, 39, 40}. We therefore examined the potential involvement of neutrophils in our system. WT and ST2^{-/-} mice were treated as above and the presence of neutrophils in the SI was examined by MPO assay and IHC. CPT-11 treatment induced neutrophil accumulation in the SI from day 2 (data not shown) along the villi and increased progressively to day 5 in the WT mice but not in the ST2^{-/-} mice (Figure 3a,b). The MPO activity in the SI of WT mice was further enhanced by the administration of IL-33. (Figure 3b). ST2^{-/-} mice did not respond to IL-33 treatment in any of the parameters evaluated (data not shown).

We then characterized the neutrophils activated by CPT-11. Neutrophils (CD11b⁺Ly6G⁺) from WT mice were highly activated in the blood 3 days after CPT-11 treatment, a time point when IL-33 production in the SI was already increased (600 ± 13 pg/ml compared to 42 ± 7 pg/ml in PBS control) and the concentration of CXCL1/KC in the serum was elevated (150 ± 9 pg/ml compared to 6 ± 1,3 in PBS control). These cells expressed the CXC chemokine receptor CXCR2 and CD62L (L-selectin) (Figure 3c-e). This time point

preceded the severe neutropenia observed at later stages of the disease (data not shown). The neutrophils accumulated in the SI of the WT mice also showed highly activated phenotype expressing CXCR2 but shedding of CD62L (Figure 3f-h). Additional IL-33-treatment led to increased percentage and activation of neutrophils, with expression of CXCR2 and CD62L in the blood from CPT-11 treated-mice (Figure 3e). CD62L expression was again reduced on the neutrophils from the SI of mice treated with CPT-11 + IL-33 compared to that on the neutrophils from mice treated with CPT-11 alone (Figure 3h). In contrast, little or no neutrophil activation was observed in the blood or SI of ST2^{-/-} mice treated with CPT-11.

To further investigate the role of neutrophils in chemotherapy-induced intestinal mucositis, we first asked whether CPT-11 could induce the production of CXC chemokines in the SI. We cultured the SI explants from WT and ST2^{-/-} mice with CPT-11, SN-38 or IL-33 and measured the production of CXCL1 and CXCL2 by ELISA. CPT-11 and SN-38 induced a significant amount of CXCL1 and CXCL2 in the SI explants from WT mice (Figure 3i,j). The levels of chemokines produced by the SI of ST2^{-/-} mice were significantly reduced compared to that of the WT mice. IL-33 alone induced a robust production of CXCL1 and CXCL2 in the SI of WT mice but not in the SI of ST2^{-/-} mice (Figure 3i,j). These data suggest that while IL-33 is a potent inducer of CXCL1 and CXCL2 in the SI explants, CPT-11 can also induce a modest production of these chemokines independently of IL-33.

To determine the relevance of these findings in neutrophil migration, we assessed neutrophil recruitment in a transwell chamber in the presence of supernatants from SI explants treated with CPT-11 or SN-38 for 24 h. Supernatants from WT SI explants treated with CPT-11 or SN-38 significantly induced the recruitment of neutrophils (Figure 3k). Supernatant from ST2^{-/-} SI explants presented a 50-60% reduction in the effectiveness to induce neutrophil recruitment. Supernatant from WT (but not ST2^{-/-}) SI explants treated with IL-33 alone also induced the recruitment of neutrophils. To confirm the active role of IL-33 in the SI supernatants, we added sST2 to the supernatant in the transwell experiment. The IL-33 decoy receptor, sST2, significantly reduced neutrophil migration attracted by the supernatants from CPT-11 or SN-38-treated WT SI (Figure 3l).

Together these results demonstrate that neutrophils play a key role in the CPT-11-induced mucositis, at least partly, via the IL-33/ST2-mediated elevation of the chemokines production and chemokine receptors expression.

IL-33 blockade ameliorates CPT-11-induced intestinal mucositis

We next investigated whether the reduced mucositis in the ST2^{-/-} mice can be reproduced by blocking endogenous IL-33 using an anti-IL-33 antibody and sST2. WT mice were treated with CPT-11 for 4 consecutive days with or without daily injection of anti-IL-33 or sST2. Both anti-IL-33 and sST2 significantly reduced body weight loss and clinical score compared to PBS injected control mice (Figure 4a,b). The disease amelioration was accompanied by a reduction in tissue injury and signs of hemorrhage and congestion (Figure 4c), with reduced villi shortening (Figure 4d). Neutrophil accumulation and the production of CXC and CC chemokines CXCL1, CXCL2 and CCL2 in the SI were also significantly reduced in the anti-IL33- and sST2-treated mice compared to PBS-treated control mice

(Figure 4e-h). These data therefore confirmed the in vivo endogenous role of IL-33 in driving disease and tissue damage in CPT-11-induced intestinal mucositis.

Neutrophil depletion attenuates CPT-11-induced intestinal mucositis

We next investigated the effect of neutrophil depletion on CPT-11-induced intestinal mucositis. WT mice were treated with CPT-11 and then injected with anti-Ly6G antibody. The antibody effectively depleted neutrophils (CD11b⁺ CXCR2⁺) in the SI as analyzed by FACS (up to 80%, Supplementary Figure S2a online). An intermediary dose of anti-Ly6G antibody (100 µg, every 2 days) was used so as to avoid development of early severe neutropenia in the present experimental setting³⁸. Neutrophil depletion significantly prevented the body weight loss and clinical disease in the CPT-11-treated and CPT-11 plus IL-33-treated WT mice compared to IgG-treated control mice (Figure 5a,b). The disease attenuation achieved by anti-Ly6G antibody was accompanied by a significant reduction of the SI histopathology in the antibody-treated mice (Figure 5c,d). Furthermore, neutrophil accumulation (Supplementary Figure S2b online) and the production of CXCL1, CXCL2, CCL2 and IL-33, were also significantly reduced in the anti-Ly6G treated mice (Supplementary Figure S2c-f online). It may be that the accumulated activated neutrophils could cause further epithelial damage releasing these chemokines and IL-33.

To visualize neutrophil migration, we performed intra-vital microscopy to assess the rolling and adhesion of leukocytes in the mesenteric microvasculature in WT and ST2^{-/-} mice treated with CPT-11. No significant difference in the rolling of the leukocytes was observed between WT and ST2^{-/-} mice (Figure 5e). In contrast, significantly more firm adhesion of leukocytes to the mesenteric endothelial veins was found in the WT mice treated with CPT-11 compared to untreated mice (Figure 5f). The increased cellular adhesion was not evident in the microvasculature of the ST2^{-/-} mice (Figure 5f,g and Supplementary Video S1-4 online). The leukocyte adhesion in the CPT-11-treated WT mice peaked on day 2 of treatment, coinciding with the onset of clinical signs and leukopenia.

CXCR2 is known to be an important receptor involved in neutrophil arrest in vivo⁸. To further confirm the role of neutrophil migration in CPT-11-induced mucositis, we blocked the chemokine receptor CXCR2 in vivo using a specific antagonist, DF-2156A, which has been used to inhibit CXCR2 function on neutrophils and the migration of these cells⁴¹. WT mice were treated with CPT-11 alone or with IL-33 as above. The mice were administered orally with a daily dose of DF-2156A. DF-2156A significantly reduced intestinal mucositis induced by CPT-11 and CPT-11 + IL-33 (Supplementary Figure S3a online). DF-2156A also effectively blocked neutrophil infiltration in the SI (Supplementary Figure S3b online). Furthermore DF-2156A markedly reduced the production of CXCL1, CXCL2 and IL-33 by the SI of CPT-11-treated and CPT-11 + IL-33-treated mice (Supplementary Figure S3c-e online). Significant reduction of the SI histopathology was also observed in DF2156A-treated mice compared to PBS-treated control mice (Supplementary Figure S3f, g online). These results further indicate the critical role of neutrophil migration in the CPT-11-induced mucositis.

Collectively, these data demonstrate that neutrophils play an important role in the onset and outcome of intestinal mucositis induced by CPT-11. Importantly, IL-33 participates in the

cascade of events leading to neutrophil adhesion and accumulation in the SI during chemotherapy-induced mucositis.

IL-33 targeting attenuates intestinal mucositis and extends effective tumour chemotherapy

The important role of IL-33 in CPT-11-induced mucositis prompted us to investigate if IL-33 blockade would enable a longer period of treatment with this cytotoxic drug against tumour, using a murine model of ectopic colon carcinoma induced by CT26 cells. WT and ST2^{-/-} mice were injected s.c. with CT26 cells and CPT-11 treatment began 48 h later when the transplanted tumour was visible and/or palpable. The schedule of CPT-11 treatment was set to the minimum dose (45 mg/kg for 5 days) able to reduce CT26-tumour growth without being lethal to WT mice for at least 21 days from the start of treatment. The dose was reduced by half (22.5 mg/kg for 5 days) when the WT mice presented signs of mucositis; and the dose was reduced to half again (11.5 mg/kg) until day 18-21 post CT26 transplant. There was no significant difference in the rate of tumour growth and mortality between WT and ST2^{-/-} mice without CPT-11 treatment (Figure 6a and Supplementary Figure S4a online). WT mice treated with CPT-11 showed significant reduction in tumour size and survival. However these mice developed severe intestinal mucositis and the treatment was withdrawn on day 5. In contrast, ST2^{-/-} showed no obvious sign of mucositis and continued to receive tapering doses of CPT-11. This prolonged continuous CPT-11 treatment resulted in further reduction of tumour size compared to that of CPT-11-treated WT mice. The beneficial outcome of CPT-11 treatment in the ST2^{-/-} mice was reflected in the significantly milder clinical score and reduced weight loss in these mice compared to the WT mice (Figure 6a and Supplementary Figure S4a online).

We next investigated the effect of IL-33 blockade with anti-IL-33 antibody. BALB/c mice were transplanted with CT26 and treated with CPT-11 as above. Some mice also received a daily i.p. injection of anti-IL-33 or IgG isotype control from day 2 to 12. As expected, mice given CPT-11 alone showed significantly reduced tumour size but severe mucositis. The treatment was withdrawn on day 6. In contrast, mice administered with anti-IL-33 developed mild mucositis and the continuous treatment with CPT-11 resulted in significantly further reduction in tumour size compared to mice given IgG control (Figure 6b and Supplementary Figure S4b online). The beneficial outcome of anti-IL-33 injection was also evident in the reduced clinical score and body weight loss (Figure 6b).

To confirm the beneficial effect of IL-33 blockade, we also treated mice with sST2. WT mice were injected with CPT-11 as above and then received a daily i.p. injection of sST2 from day 2 to 12. Mice given sST2 developed little or no mucositis and were able to receive continuous CPT-11 treatment. This treatment resulted in significant further reduction of tumour size compared to the control mice given PBS (Figure 6c and Supplementary Figure S4c online). The relative absence of mucositis in the sST2-treated mice was also reflected in the reduced clinical score (reduced diarrhea) and body weight loss compared to PBS-treated mice (Figure 6c).

Collectively, these data demonstrate that IL-33 blockade effectively reduces mucositis and enables prolonged CPT-11 treatment leading to a significant beneficial outcome of chemotherapy.

DISCUSSION

We demonstrate here that IL-33 mediates CPT-11-induced mucositis through the local production of CXCL1 and CXCL2, which recruits neutrophils to the site of inflammation causing tissue damage in the small intestine (Figure 7). Furthermore, blockade of the IL-33/ST2 pathway or neutrophil recruitment confers protection and tissue preservation. Importantly, IL-33 neutralization enables extended and effective chemotherapy in CT26-tumour-bearing mice, suggesting that the IL-33/ST2 pathway is a novel therapeutic target to alleviate mucosal damage leading to a beneficial outcome of cancer chemotherapy.

IL-33 is rapidly produced by small intestine epithelial cells (epT) in the villi and crypts following exposure to CPT-11 in vivo and in vitro. IL-33 functions as a prototypic ‘alarmin’, released upon cellular damage, stress and necrosis, and may serve as a danger signal to alert the host of a local imbalance, such as trauma or infection^{21, 42}. It is likely that both inactivation and release of IL-33 take place linking between apoptosis and cell damage in many acute and chronic inflammatory diseases in which IL-33 has been detected. Gut mucosal expression of IL-33 is primarily localized to non-hematopoietic cells, particularly intestinal epT^{25, 43}. In active ulcerative colitis (UC), IL-33 is localized to, and potently expressed by, epT^{24, 43}. Moreover, IL-33 has been shown to impair intestinal barrier function, where enhanced IL-33 may favor microbial translocation that perpetuates colonic inflammation in a model of DSS-induced colitis in mice²³. We show here that CPT-11-induced IL-33 led to markedly increased bacteremia in an ST2-dependent manner. Together with the impaired intestinal barrier function, diarrhea in CPT-11-treated mice is thought to be caused by villous atrophy following crypt damage and apoptosis of absorptive cells in the small intestine^{33, 34}. Since diarrhea is one of the main drawbacks for cancer patients undergoing chemotherapy³², attenuation of IL-33/ST2-dependant mucositis might also represent a therapeutic approach to diarrhea associated to CPT-11 treatment.

We have previously shown that IL-33 contributes to the increased expression of CXCR2 on neutrophils through the up-regulation of GRK2 (G Protein-Coupled Receptor Kinase 2) following TLR4 activation in a model of poly-microbial sepsis⁴⁴. However, we did not observe any alteration in the expression of GRK2 on neutrophils harvested from the SI or blood following CPT-11 + IL-33 treatment (data not shown). This is perhaps not unexpected since, unlike sepsis, CPT-11-treatment induces neutrophil migration in the absence of massive infection. Bacteremia is related to epithelial damage late in the chemotherapy⁹. The role of neutrophils in chemotherapy-induced mucosal damage was hitherto unknown^{1, 2}. We demonstrate here that neutrophil depletion and CXCR2 blockade represent an efficient strategy to reduce the mucosal injury following epT release of IL-33 and pro-inflammatory cytokines.

Local production of IL-33 may induce a rapid release of pro-inflammatory mediators such as IL-1 β , IL-6, TNF α and chemokines by a variety of innate immune cells including neutrophils, macrophages and mast cells^{16, 22, 45}. During active UC and SAMP enteritis (using SAMP1/YitFc mice, which develop spontaneous ileitis similar in many features to human Crohn’s disease), IL-33 is markedly up-regulated in colonic epTs and similar gut mucosal cells also express the receptor ST2, suggesting that IL-33 may act in an autocrine/

paracrine fashion to amplify the inflammatory response in the context of SI inflammation²⁵. ST2 is present on the surface of neutrophils, although IL-33 is not directly involved in their recruitment⁴⁴. However, the robust production of the chemokines CXCL1 and CXCL2 indicates that IL-33 strongly contributes to the recruitment of neutrophils to the site of injury. Thus strategies targeting the IL-33-CXC-Neutrophils axis may help to limit collateral damage during responses to sterile injury by allowing neutrophils to remain intravascular as they navigate through healthy tissue to sites of injury⁴⁶. Even if blood neutropenia might compromise the host immune response at later time points, the early accumulation of neutrophils in the SI mucosa is a key event in driving tissue damage and disease during cancer chemotherapy. It should be noted that treatment with rmIL-33 alone without CPT-11 did not lead to significant pathology. It is likely that epithelial damage induced by the cytotoxic effect of CPT-11 is necessary for the infiltration of neutrophil migration from the circulation to the inflammatory site. Alternatively, IL-33 may have to synergize with other mediators released by CPT-11-activated epT to cause the damage in the SI. These potential accessory mediators remain to be defined.

Although many studies have addressed different strategies to enhance the effectiveness of CPT-11 and other compounds in reducing tumour growth, little attempt was made to alleviate mucosal damage and improve the duration and efficiency of the chemotherapy^{3, 6, 14, 33, 34, 47}. Jovanovic and colleagues^{48, 49} reported a modest reduction in tumour growth in a model of 4T1 mammary carcinoma in ST2^{-/-} mice as compared to WT mice, suggesting that IL-33 may contribute to tumor growth⁴⁸. We did not observe a significant difference in tumour growth between CT26-bearing WT and ST2^{-/-} mice (Figure 6). This discrepancy could be due to the different type of tumour used.

sST2 treatment appeared to be more effective than anti-IL-33 in reducing mucositis, even though both treatments conferred significant protective effects in WT mice. However, this difference could be due to the suboptimal dose of anti-IL-33 antibody used (25 µg/mouse). The therapeutic basis and potential for the IL-33/ST2 blockade reside in the fact that IL-33 is released by epithelial cells as an ‘alarmin’ in response to injury, while other cells in the epithelia may produce IL-33 in chronic IBD patients^{22, 23, 25, 50}. Recent data of adult and pediatric UC and CD (Crohn’s disease) patients demonstrate that specific IL-33 and ST2 gene polymorphisms confer an increased risk of developing IBD (both UC and CD), reinforcing the involvement of the IL-33/ST2 axis in the onset of intestinal inflammation⁵¹.

In summary, we report here a pivotal role of IL-33 in mediating mucosal damage during cancer chemotherapy and that IL-33 blockade leads to a beneficial outcome of chemotherapy in a murine model of carcinoma. Importantly, IL-33 is found in considerable levels in the mucosa of IBD patients^{24, 52}. Our results therefore suggest that inhibition of the IL-33/ST2 pathway may represent a novel approach to limit inflammatory mucosal damage and thus improve the effectiveness of chemotherapy.

METHODS

Animals

BALB/c mice were purchased from Harlan-Olac, UK. BALB/c *St2^{-/-}* mice⁵³ were bred and maintained at the University of Glasgow, UK. All experiments were performed in accordance with the UK Home Office guidelines. Mice under procedure were kept in polyethylene boxes with free access to soft food and water, and subjected to 12 h light–dark cycles.

Reagents and antibodies

Irinotecan hydrochloride (CPT-11, Camptosar®) and SN-38 (7-Ethyl-10-hydroxycamptothecin) were purchased from Sigma-Aldrich. Recombinant murine IL-33 (rmIL-33) was obtained from Biolegend. Mouse IL-33 MAb (Clone 396118) and Isotype control were purchased from R&D Systems. Purified Rat anti-mouse Ly6G (clone 1A8) and Isotype control were purchased from BD Biosciences. Recombinant murine sST2 was generated and purified from HEK293T cells at VIB Protein Service Facility, VIB Inflammation Research Center, Ghent, Belgium. DF-2156A was obtained from Dompé S.p.A., L'Aquila, Italy.

Cell line

The human enterocyte-like cell line Caco-2 (ATCC® HTB-37™) and the CT26 (colon carcinoma from BALB/c, CT26.WT, ATCC® CRL-2638™) were obtained from ATCC (LGC Standards, UK) and maintained in high-glucose Dulbecco's modified Eagle medium (DMEM) (Gibco-BRL, Life Technologies) supplemented with 10% fetal calf serum (FCS) (LONZA), 1% (vol/vol) HEPES (Gibco-BRL), 1% (vol/vol) penicillin-streptomycin (Gibco-BRL), and 2 mM L-glutamine (Gibco-BRL). All cell cultures were carried out in 5% CO₂ in a humidified atmosphere at 37°C. Cells were seeded at high density in T75 tissue culture flasks (Corning) and grown to 90 % confluence. Before each experiment, culture medium and dead cells were aspirated off, and the live cells were washed 3x with FCS-free culture medium. Cells were detached using 0.5% Trypsin-EDTA (Sigma-Aldrich), counted in Trypan blue dye and used as indicated. Caco-2 cells monolayers were cultured for 48 h (100% confluence) and incubated with CPT-11 (Sigma-Aldrich) or SN-38 (Sigma-Aldrich) dissolved in DMSO (Sigma-Aldrich) then in supplemented medium (final DMSO concentration 0.2%) using 24 well culture plates (Corning) at 1×10⁶ cells/ml. CT26 cells were washed twice in HBSS (Hanks' Balanced Salt solution, Sigma Aldrich) to remove FCS contamination before subcutaneous injection in mice. Cell viability was verified by the MTT assay (Sigma-Aldrich). Briefly, cells were incubated with 300 µl MTT-containing RPMI medium (0.1 mg/ml MTT in serum-free medium) for 4 h. Medium was removed, and the formazan crystal formed in living cells was dissolved in 100 µl DMSO per well. The relative viability (%) was calculated based on absorbance at 550 nm using a microplate reader. Viability of non-treated control cells was arbitrarily defined as 100%

Induction of experimental intestinal mucositis

Experimental intestinal mucositis in mice was based on a model previously described by Ikuno et al.³⁴ and Melo et al.¹⁰ with some modifications. Briefly, vehicle (45 mg/ml of sorbitol NF powder, 0.9 mg of lactic acid, USP and DPBS, pH 3.5-3.8) or CPT-11 (60 mg/kg) was administered intraperitoneally (i.p.), for two (mild mucositis) or four (severe mucositis) consecutive days (from day 0 to day 3)⁵⁴. Some mice were also treated i.p. with IL-33 (200 ng, 30 min before each CPT-11 injection), anti-IL-33 (25 µg, daily, s.c.), anti-Ly6G (100 µg, every 2 days, s.c.), sST2 (100 µg, daily, s.c.), DF-2156A (10 mg/kg, orally daily), PBS or filtered water. On days 2 or 4, mice were culled in a CO₂ inhalation chamber. Blood was taken from the cava vein for leukocyte counts, DNA purification (sterile tubes) or serum preparation in heparinized tubes. SI was perfused, dissected, washed, measured and stored at -20°C for cytokine measurement by ELISA or at -80°C for qPCR analysis. In some experiments, SI was used for histopathological analysis or digested for FACS analysis.

CT26 tumour induction

Mice were injected subcutaneously in the shaved right flank with CT26 cells at 1×10^6 / 50 µl. When the tumour had grown to 0.1 - 0.2 cm (palpable tumours, routinely on day 2), mice were injected i.p. with 200 µl of CPT-11 (45 mg/kg/daily). The dose of CPT-11 was reduced to half of the initial dose for mice that had lost ~15% of body weight. The size of tumour was monitored daily with a caliper. The tumour size was calculated and expressed as the average tumour diameters in cm \pm SEM. Mice were culled when appeared moribund or the tumour size reached 1.2 cm diameter.

Clinical score

The severity of diarrhea and body weight loss was monitored throughout the experimental periods. The severity of the diarrhea was scored as described by Kurita et al.⁴⁷ as follows: 0, normal, normal stool or absent; 1, slight, slightly wet and soft stool; 2, moderate, wet and unformed stool with perianal staining of the coat; and 3, severe, watery stool with perianal staining of the coat.

Histopathological analysis

The SI was perfused, dissected, washed in HBSS, fixed in 4% (v/v) neutral-buffered formalin (Merck), dehydrated and embedded in paraffin. The tissues were cut into 5 µm sections, stained with Hematoxylin-Eosin (H&E) or Periodic acid-Schiff (PAS) and examined with a Nikon Eclipse E400 microscope at x200 or x400 magnification. The severity of SI inflammation (leukocyte infiltration and tissue damage in the intestinal parenchyma) was assessed by a semi-quantitative score (0-4) in a blinded fashion. The severity of mucositis was graded using the following criteria as previously described⁵⁵: grade 0, no lesion; grade 1, <10% crypts contain individual necrotic cells, grade 2, >10% crypts contain necrotic cells but the crypt architecture is intact; grade 3, >10% crypts contain necrotic cells showing focal loss of crypt architecture (<20%), villi are shortened, and variable hypertrophy/hyperbasophilia apparent in the remaining crypt cells; grade 4, same as grade 3 except that the loss of crypt architecture and villous shortening are more extensive. Intestinal villus and crypt lengths were measured by an optical scale under $\times 200$.

magnification, and villus-to-crypt length ratios calculated. Goblet cells were counted per hemi crypt/villus axis. A total of 25 crypts or hemi crypt/villus axis was counted in at least five different SI slides per experimental group.

Immunohistochemistry

The immunohistochemistry demonstration of IL-33 or Myeloperoxidase (MPO) protein in the SI was performed on paraffin sections of formalin-fixed samples using a mouse anti-IL-33 MAb (Clone 396118), Rat IgG2A, Anti-Annexin V polyclonal antibody (Abcam, ab14196), Rabbit IgG, and Human/Mouse Myeloperoxidase Affinity Purified Polyclonal Ab, Goat IgG (All from R&D systems unless otherwise specified). De-paraffinized sections were incubated with anti-IL-33, anti-Annexin V or anti-MPO antibody (diluted 1:600-1:1000 in 0.2% bovine serum albumin and 1:25 dilution of mouse serum) for 90 min at room temperature. The bound antibody was visualized by an avidin–biotin–peroxidase method (Vectastain Elite kit, Vector Laboratories) and developed with 3,3'-diaminobenzidine (DAB; Sigma-Aldrich) in the presence of H₂O₂ as the chromogen. SI samples served as negative controls by omission of the primary antibody during otherwise identical incubations. SI samples from different control groups served as a further internal control. Staining was assessed by light microscopy (x200, x400).

Vascular permeability and neutrophil accumulation

The SI was perfused, washed and removed at the indicated time points. The extravasation of Evans Blue dye into the SI was used as an index of increased vascular permeability, as previously described⁵⁶. Results are presented as the amount of Evans Blue in microgram per 100 mg of tissue in 1 ml. The extent of neutrophil accumulation in the SI was measured by myeloperoxidase (MPO) activity as previously described⁵⁶. Results are expressed as relative units (OD 492 nm) and corrected for the activity of other peroxidases not inhibited by 3-amino-1,2,4-triazole.

Western blotting analysis

Cells were lysed in RIPA buffer (Thermo Scientific) containing protease inhibitors (Roche). Supernatants were used as total lysates. Protein concentrations were estimated by the BCA protein assay (Pierce). Supernatants were then boiled in reducing SDS sample buffer and 30 µg of protein lysate per lane were run through NuPAGE® Novex® 4-12% Bis-Tris Protein Gels (Life Technologies) and transferred to Hybond ECL membranes (GE Healthcare). Membranes were blocked for 1 h in 5% non-fat dried milk in DPBS and incubated overnight with the appropriate primary antibody at 4°C. Membranes were then washed in DPBS/Tween 20 and incubated with the appropriate secondary antibody. Both primary and secondary antibodies were diluted in 5% non-fat dried milk in DPBS. Detection was performed by ECL Western Blotting Detection Reagents (GE Healthcare). Antibodies against cleaved PARP (Asp214, mAb), Caspase 9 (mAb) and all secondary antibodies were obtained from Cell Signaling Technologies. Caspase-3 (rabbit polyclonal) and Bax (mAb) antibodies were obtained from Santa Cruz Biotechnology.

ELISA

The concentrations of IL-33, sST2, IL-8, CXCL1, CXCL2, CCL2 was analyzed by ELISA (all reagents were from R&D Systems) on sera, tissue or cell culture supernatants according to the manufacturer's instructions. The sensitivity of the assay was <20 pg/ml.

Intravital microscopy

An intra-vital microscope (ECLIPSE 50i, Nikon) with a 20x objective lens was used to examine the mesenteric microcirculation on day 2 post CPT-11 injections (60 mg/kg) in selected post-capillary venules within 40–60 μ m. A digital camera (DS-Qi1MC, Nikon) was used to project the images onto a computer monitor, and the images were recorded for playback analysis with an Imaging Software (Nikon, Kawasaki). To measure the leukocyte-endothelial cell interactions, the fluorescent marker Rhodamine 6G (Sigma-Aldrich) was injected in the caudal vein (in a single bolus of 0.15 mg/kg) immediately before measurements. The flux of rolling cells was measured as the number of cells that passed by a given point per min. A leukocyte was considered to be adherent if it remained stationary for at least 30 seconds. Total leukocyte adhesion was quantified as the number of adherent cells in the intravascular space within an area of 100 μ m.

Isolation of epithelial cells (epT) from the SI

Small intestine from naïve BALB/c mice was harvested, cut in 5 cm-long pieces and the luminal surface exposed. Samples were incubated in PBS-EDTA (30 mM) for 15 min, at 37°C under mild agitation to remove the epithelial layer. Epithelial cell preparation was filtered through 70 μ m mesh, washed in RPMI-10% FCS, and filtered again. Epithelial cells were counted and 2×10^6 cells were cultured in RPMI-10% FCS for 6 h with CPT-11 or RPMI with 0,1% DMSO as vehicle control.

Preparation and culture of SI explants

SI was opened longitudinally and washed thoroughly in sterile DPBS supplemented with 2% FCS and 1% penicillin/streptomycin. Fat tissue was removed and segments with peyer patches were excluded. Three to five segments from terminal duodenum of 1 cm in length per mice were placed in 24 well culture plates (Corning) containing fresh RPMI 1640 (Life Technologies) supplemented with 10% FCS, 1% penicillin/streptomycin and incubated at 37°C for 24 h. Segments were kept with the luminal surface exposed to the medium. Reagents of interest were added to the culture for 24 h. DMSO concentration was used at 0.2%. Supernatants were then harvested, centrifuged at $13,000 \times g$, and stored at -20°C until used. Some explants were pre-incubated with 10 μ g/ml sST2 for 40 min at 37°C.

Neutrophil isolation and chemotaxis assay

Neutrophils were purified from BALB/c bone marrow by positive selection using a Ly6G isolation kit (Miltenyi Biotec.). Ly6G⁺ cells were re-suspended in chemotaxis buffer (0.5% BSA in RPMI 1640) and neutrophil migration was assayed in 24-well sterile polystyrene plates with transwell permeable supports containing 5 μ m pore size polycarbonate membranes (Corning). mCXCL2 (10 ng/ml, Peprotech) that was able to induce the recruitment of 1×10^5 purified Ly6G⁺ neutrophils per ml to the lower chamber after 3 h was

used as positive control (data not shown). Freshly collected supernatants from SI explants were added in the lower chamber (600 µl/well). As negative control, chemotaxis buffer (BSA + RPMI) only was added. Neutrophils ($1 \times 10^6/100 \mu\text{l}$) were added in the top chamber. The plate was then incubated for 3 h at 37°C in 5% CO₂. Migrated neutrophils were recovered from the lower chamber, centrifuged, re-suspended and counted under light microscopy ($\times 400$) using a Neubauer haemocytometer.

Isolation of SI leukocytes

The SI of mice were perfused, removed and washed in HBSS. Fat tissue and peyer patches were removed; the SI was opened longitudinally, washed in 2% FCS in HBSS, and cut into 0.5 cm sections. Tissue was then placed in 10 ml HBSS/2% FCS and shaken for 15 min at 37°C, and the supernatant discarded. Freshly prepared calcium/magnesium-free HBSS (10 ml, Life Technologies) containing 2 mM EDTA (Sigma-Aldrich) was then added. The tube was placed in a shaking incubator for 15 min at 37°C, and the supernatant discarded. Calcium/magnesium-free HBSS (10 ml) was then added, the tube was shaken, and the supernatant discarded. This step was repeated, and the remaining tissue was digested with 1.25 mg/ml collagenase D (Roche Diagnostic Systems, Mannheim, Germany), 1 mg/ml Dispase (Life Technologies), and 0.5 mg/ml DNase (Sigma-Aldrich) in complete RPMI 1640 for 30–40 min in a shaker at 37°C until complete digestion of the tissue. The final supernatant was passed twice through 100 µm cell strainers (Falcon). Cells were centrifuged, washed and counted in Trypan blue.

Flow cytometry

Leukocytes ($\sim 1 \times 10^6$ cells/tube) were stained with DAPI (cell viability), anti-CD45-Pacific Blue, anti-F4/80-FITC, anti-CD11b-PercP Cy5.5, anti-Ly6G-APC, anti-CXCR2-PE (all R&D Systems), anti-CD62L-FITC, anti-GRK2-FITC, anti-Cytokeratin (C-11)-FITC (Abcam), anti-IL-33-PE (R&D Systems) and isotype controls (BD Biosciences), following the manufacturer's protocols. IL-33 production by CD45⁺ Cytokeratin⁺ epT cells was determined after stimulation with PMA (50 ng/ml) and ionomycin (1 µg/ml) in the presence of GolgiStop™ and permeabilization of the cells (Cytofix/Cytoperm, BD Biosciences). Cells were acquired using a Beckman Coulter CyAn™ ADP (Beckman Coulter, USA). Gating strategy (Supplementary Figure S5 online) and analysis were performed using the FlowJo® software (treeStar Software, USA).

Real-time PCR

For RNA extraction, SI was isolated and preserved in RNAlater (Qiagen). The tissue was homogenized in TRIzol reagent (Sigma-Aldrich) and RNA was extracted according to standard protocol (RNeasy kit, Qiagen). For quantitative real-time PCR analysis, cDNA was amplified using M-MLV Reverse Transcriptase (Promega). Relative quantities of mRNA was determined using SYBR Green PCR Master Mix (Applied Biosystems) and by the comparative threshold cycle method provided by the manufacturer for the ABI Prism 7700/7900HT Sequence Detection System. Primers were: mouse *bax*, F 5'-TTG CTG ATG GCA ACT TCA ACT GGG-3' and R 5'-TGT CCA GCC CAT GAT GGT TCT GAT-3'. Mouse *casp3*, F 5'-TGG CAA CGG AAT TCG AGT CCT TCT -3' and R 5'-TGA GCA

TGG ACA CAA TAC ACG GGA-3'. Relative expression levels were calculated as Ct values by normalizing Ct values of target genes to Ct values of hypoxanthine phosphoribosyl transferase-1 (*hprt1*). Data are presented as relative % of expression. For the detection of Eubacteria, blood samples were collected from mice on day 4 using sterile material (endotoxin free / pyrogen free, Costar) and total DNA extracted using the DNeasy Blood & Tissue Kit (Qiagen). A standard curve was prepared using purified DNA from *E.coli* (concentration range of 1 pg to 1 µg/ml). The amount of Eubacteria DNA was determined using SYBR Green PCR Master Mix (Applied Biosystems) with the standard curve as a reference for the quantification of DNA per sample. Primers: UniF340, ACTCCTACGGGA GGCAGCAGT; UniR514, ATTACCGCGGCTGCTGGC.

Statistical analysis

Results are shown as means ± SEM. Differences were compared by using one-way analysis of variance (ANOVA) followed by Student-Newman-Keuls or Bonferroni post hoc analysis using the Graph Prism Software 4.0. Tumour size and body weight were analyzed using two-way analysis of variance (ANOVA). All data are representative of at least two experiments. Results with a P<0.05 were considered significant.

Supplementary Material

Refer to Web version on PubMed Central for supplementary material.

Acknowledgments

This work was supported by the Wellcome Trust and the Medical Research Council, UK (to F.Y.L. and G.J.G.); the Belgian Federation against Cancer, MRP-Group-ID, IWT-SBO and FWO programs (to R.B.); CNPq, FAPEMIG and CAPES, Brazil (to M.M.T. and G.B.M.); and the European Community's Seventh Framework Programme [FP7-2007-2013] under grant agreement n°HEALTH-F4-2011-281608 (to M.M.T. and G.J.G.). We thank Mr. Iain MacMillan (Veterinary School, University of Glasgow) for help with histology and IHC.

REFERENCES

1. Sonis ST. The pathobiology of mucositis. *Nat Rev Cancer*. 2004; 4(4):277–284. [PubMed: 15057287]
2. Sonis ST. A biological approach to mucositis. *J Support Oncol*. 2004; 2(1):21–32. discussion 35–26. [PubMed: 15330370]
3. Mathijssen RH, van Alphen RJ, Verweij J, Loos WJ, Nooter K, Stoter G, et al. Clinical pharmacokinetics and metabolism of irinotecan (CPT-11). *Clin Cancer Res*. 2001; 7(8):2182–2194. [PubMed: 11489791]
4. Hebbar M, Ychou M, Ducreux M. Current place of high-dose irinotecan chemotherapy in patients with metastatic colorectal cancer. *J Cancer Res Clin Oncol*. 2009; 135(6):749–752. [PubMed: 19343364]
5. Paduch R, Kandefer-Szerszen M, Piersiak T. The importance of release of proinflammatory cytokines, ROS, and NO in different stages of colon carcinoma growth and metastasis after treatment with cytotoxic drugs. *Oncol Res*. 2010; 18(9):419–436. [PubMed: 20524400]
6. Kawato Y, Aonuma M, Hirota Y, Kuga H, Sato K. Intracellular roles of SN-38, a metabolite of the camptothecin derivative CPT-11, in the antitumor effect of CPT-11. *Cancer Res*. 1991; 51(16):4187–4191. [PubMed: 1651156]
7. Logan RM, Stringer AM, Bowen JM, Gibson RJ, Sonis ST, Keefe DM. Serum levels of NFκB and pro-inflammatory cytokines following administration of mucotoxic drugs. *Cancer Biol Ther*. 2008; 7(7):1139–1145. [PubMed: 18535404]

8. Logan RM, Stringer AM, Bowen JM, Gibson RJ, Sonis ST, Keefe DM. Is the pathobiology of chemotherapy-induced alimentary tract mucositis influenced by the type of mucotoxic drug administered? *Cancer Chemother Pharmacol.* 2009; 63(2):239–251. [PubMed: 18351341]
9. Leitao RF, Brito GA, Oria RB, Braga-Neto MB, Bellaguarda EA, Silva JV, et al. Role of inducible nitric oxide synthase pathway on methotrexate-induced intestinal mucositis in rodents. *BMC Gastroenterol.* 2011; 11:90. [PubMed: 21846355]
10. Melo ML, Brito GA, Soares RC, Carvalho SB, Silva JV, Soares PM, et al. Role of cytokines (TNF- α , IL-1 β and KC) in the pathogenesis of CPT-11-induced intestinal mucositis in mice: effect of pentoxifylline and thalidomide. *Cancer Chemother Pharmacol.* 2008; 61(5):775–784. [PubMed: 17624531]
11. Vento S, Cainelli F. Infections in patients with cancer undergoing chemotherapy: aetiology, prevention, and treatment. *Lancet Oncol.* 2003; 4(10):595–604. [PubMed: 14554236]
12. Brandi G, Dabard J, Raibaud P, Di Battista M, Bridonneau C, Pisi AM, et al. Intestinal microflora and digestive toxicity of irinotecan in mice. *Clin Cancer Res.* 2006; 12(4):1299–1307. [PubMed: 16489087]
13. Arcaroli JJ, Powell RW, Varella-Garcia M, McManus M, Tan AC, Quackenbush KS, et al. ALDH + tumor-initiating cells exhibiting gain in NOTCH1 gene copy number have enhanced regrowth sensitivity to a gamma-secretase inhibitor and irinotecan in colorectal cancer. *Mol Oncol.* 2012; 6(3):370–381. [PubMed: 22521243]
14. Finnberg N, Kim SH, Furth EE, Liu JJ, Russo P, Piccoli DA, et al. Non-invasive fluorescence imaging of cell death in fresh human colon epithelia treated with 5-Fluorouracil, CPT-11 and/or TRAIL. *Cancer Biol Ther.* 2005; 4(9):937–942. [PubMed: 16251801]
15. Schmitz J, Owyang A, Oldham E, Song Y, Murphy E, McClanahan TK, et al. IL-33, an interleukin-1-like cytokine that signals via the IL-1 receptor-related protein ST2 and induces T helper type 2-associated cytokines. *Immunity.* 2005; 23(5):479–490. [PubMed: 16286016]
16. Liew FY, Pitman NI, McInnes IB. Disease-associated functions of IL-33: the new kid in the IL-1 family. *Nat Rev Immunol.* 2010; 10(2):103–110. [PubMed: 20081870]
17. Luthi AU, Cullen SP, McNeela EA, Duriez PJ, Afonina IS, Sheridan C, et al. Suppression of interleukin-33 bioactivity through proteolysis by apoptotic caspases. *Immunity.* 2009; 31(1):84–98. [PubMed: 19559631]
18. Tominaga S. A putative protein of a growth specific cDNA from BALB/c-3T3 cells is highly similar to the extracellular portion of mouse interleukin 1 receptor. *FEBS Lett.* 1989; 258(2):301–304. [PubMed: 2532153]
19. Xu D, Chan WL, Leung BP, Huang F, Wheeler R, Piedrafita D, et al. Selective expression of a stable cell surface molecule on type 2 but not type 1 helper T cells. *J Exp Med.* 1998; 187(5):787–794. [PubMed: 9480988]
20. Kumar S, Tzimas MN, Griswold DE, Young PR. Expression of ST2, an interleukin-1 receptor homologue, is induced by proinflammatory stimuli. *Biochem Biophys Res Commun.* 1997; 235(3):474–478. [PubMed: 9207179]
21. Cayrol C, Girard J-P. The IL-1-like cytokine IL-33 is inactivated after maturation by caspase-1. *Proceedings of the National Academy of Sciences of the United States of America.* 2009; 106(22):9021–9026. [PubMed: 19439663]
22. Pastorelli L, De Salvo C, Vecchi M, Pizarro TT. The role of IL-33 in gut mucosal inflammation. *Mediators Inflamm.* 2013; 2013:608187. [PubMed: 23766561]
23. Sedhom MA, Pichery M, Murdoch JR, Foligne B, Ortega N, Normand S, et al. Neutralisation of the interleukin-33/ST2 pathway ameliorates experimental colitis through enhancement of mucosal healing in mice. *Gut.* 2012
24. Beltran CJ, Nunez LE, Diaz-Jimenez D, Farfan N, Candia E, Heine C, et al. Characterization of the novel ST2/IL-33 system in patients with inflammatory bowel disease. *Inflamm Bowel Dis.* 2010; 16(7):1097–1107. [PubMed: 20014018]
25. Pastorelli L, Garg RR, Hoang SB, Spina L, Mattioli B, Scarpa M, et al. Epithelial-derived IL-33 and its receptor ST2 are dysregulated in ulcerative colitis and in experimental Th1/Th2 driven enteritis. *Proc Natl Acad Sci U S A.* 2010; 107(17):8017–8022. [PubMed: 20385815]

26. Seidelin JB, Rogler G, Nielsen OH. A role for interleukin-33 in T(H)2-polarized intestinal inflammation? *Mucosal Immunol.* 2011; 4(5):496–502. [PubMed: 21613987]
27. Pushparaj PN, Li D, Komai-Koma M, Guabiraba R, Alexander J, McSharry C, et al. Interleukin-33 exacerbates acute colitis via interleukin-4 in mice. *Immunology.* 2013; 140(1):70–77. [PubMed: 23582173]
28. Stringer AM, Gibson RJ, Bowen JM, Logan RM, Ashton K, Yeoh AS, et al. Irinotecan-induced mucositis manifesting as diarrhoea corresponds with an amended intestinal flora and mucin profile. *Int J Exp Pathol.* 2009; 90(5):489–499. [PubMed: 19765103]
29. Stringer AM, Gibson RJ, Logan RM, Bowen JM, Yeoh AS, Laurence J, et al. Irinotecan-induced mucositis is associated with changes in intestinal mucins. *Cancer Chemother Pharmacol.* 2009; 64(1):123–132. [PubMed: 18998135]
30. Lima-Junior RC, Figueiredo AA, Freitas HC, Melo ML, Wong DV, Leite CA, et al. Involvement of nitric oxide on the pathogenesis of irinotecan-induced intestinal mucositis: role of cytokines on inducible nitric oxide synthase activation. *Cancer Chemother Pharmacol.* 2012; 69(4):931–942. [PubMed: 22101361]
31. Sultani M, Stringer AM, Bowen JM, Gibson RJ. Anti-inflammatory cytokines: important immunoregulatory factors contributing to chemotherapy-induced gastrointestinal mucositis. *Chemother Res Pract.* 2012; 2012:490804. [PubMed: 22973511]
32. Stein A, Voigt W, Jordan K. Chemotherapy-induced diarrhea: pathophysiology, frequency and guideline-based management. *Ther Adv Med Oncol.* 2010; 2(1):51–63. [PubMed: 21789126]
33. Guffroy M, Hodge T. Re:Irinotecan (CPT-11) and characteristic mucosal changes in the mouse ileum and cecum. *J Natl Cancer Inst.* 1996; 88(17):1240–1241. [PubMed: 8780636]
34. Ikuno N, Soda H, Watanabe M, Oka M. Irinotecan (CPT-11) and characteristic mucosal changes in the mouse ileum and cecum. *J Natl Cancer Inst.* 1995; 87(24):1876–1883. [PubMed: 7494232]
35. Bodey GP. Antibiotic therapy of infections in patients undergoing cancer chemotherapy. *Antibiot Chemother.* 1974; 18:49–88. [PubMed: 4463826]
36. Le H, Kim W, Kim J, Cho HR, Kwon B. Interleukin-33: a mediator of inflammation targeting hematopoietic stem and progenitor cells and their progenies. *Front Immunol.* 2013; 4:104. [PubMed: 23653627]
37. Su Z, Lin J, Lu F, Zhang X, Zhang L, Gandhi NB, et al. Potential autocrine regulation of interleukin-33/ST2 signaling of dendritic cells in allergic inflammation. *Mucosal Immunol.* 2013; 6(5):921–930. [PubMed: 23299617]
38. Blijlevens NM, Logan RM, Netea MG. The changing face of febrile neutropenia-from monotherapy to moulds to mucositis. *Mucositis: from febrile neutropenia to febrile mucositis. J Antimicrob Chemother.* 2009; 63(Suppl 1):i36–40. [PubMed: 19372181]
39. Soares PM, Lopes LO, Mota JM, Belarmino-Filho JN, Ribeiro RA, Souza MH. Methotrexate-induced intestinal mucositis delays gastric emptying and gastrointestinal transit of liquids in awake rats. *Arq Gastroenterol.* 2011; 48(1):80–85. [PubMed: 21537548]
40. Fijlstra M, Rings EH, Verkade HJ, van Dijk TH, Kamps WA, Tissing WJ. Lactose maldigestion during methotrexate-induced gastrointestinal mucositis in a rat model. *Am J Physiol Gastrointest Liver Physiol.* 2011; 300(2):G283–291. [PubMed: 21088238]
41. Bertini R, Barcelos LS, Beccari AR, Cavalieri B, Moriconi A, Bizzarri C, et al. Receptor binding mode and pharmacological characterization of a potent and selective dual CXCR1/CXCR2 non-competitive allosteric inhibitor. *Br J Pharmacol.* 2012; 165(2):436–454. [PubMed: 21718305]
42. Moussion C, Ortega N, Girard JP. The IL-1-like cytokine IL-33 is constitutively expressed in the nucleus of endothelial cells and epithelial cells in vivo: a novel ‘alarmin’? *PLoS One.* 2008; 3(10):e3331. [PubMed: 18836528]
43. Kobori A, Yagi Y, Imaeda H, Ban H, Bamba S, Tsujikawa T, et al. Interleukin-33 expression is specifically enhanced in inflamed mucosa of ulcerative colitis. *J Gastroenterol.* 2010; 45(10):999–1007. [PubMed: 20405148]
44. Alves-Filho JC, Sonogo F, Souto FO, Freitas A, Verri WA Jr. Auxiliadora-Martins M, et al. Interleukin-33 attenuates sepsis by enhancing neutrophil influx to the site of infection. *Nature medicine.* 2010; 16(6):708–712.

45. Oboki K, Ohno T, Kajiwara N, Arae K, Morita H, Ishii A, et al. IL-33 is a crucial amplifier of innate rather than acquired immunity. *Proc Natl Acad Sci U S A*. 2010; 107(43):18581–18586. [PubMed: 20937871]
46. McDonald B, Pittman K, Menezes GB, Hirota SA, Slaba I, Waterhouse CC, et al. Intravascular danger signals guide neutrophils to sites of sterile inflammation. *Science*. 2010; 330(6002):362–366. [PubMed: 20947763]
47. Kurita A, Kado S, Kaneda N, Onoue M, Hashimoto S, Yokokura T. Alleviation of side effects induced by irinotecan hydrochloride (CPT-11) in rats by intravenous infusion. *Cancer Chemother Pharmacol*. 2003; 52(5):349–360. [PubMed: 12904895]
48. Jovanovic I, Radosavljevic G, Mitrovic M, Juranic VL, McKenzie AN, Arsenijevic N, et al. ST2 deletion enhances innate and acquired immunity to murine mammary carcinoma. *Eur J Immunol*. 2011; 41(7):1902–1912. [PubMed: 21484786]
49. Milovanovic M, Volarevic V, Radosavljevic G, Jovanovic I, Pejnovic N, Arsenijevic N, et al. IL-33/ST2 axis in inflammation and immunopathology. *Immunol Res*. 2012; 52(1-2):89–99. [PubMed: 22392053]
50. Salas A. The IL-33/ST2 axis: yet another therapeutic target in inflammatory bowel disease? *Gut*. 2013; 62(10):1392–1393. [PubMed: 23315502]
51. Latiano A, Palmieri O, Pastorelli L, Vecchi M, Pizarro TT, Bossa F, et al. Associations between Genetic Polymorphisms in IL-33, IL1R1 and Risk for Inflammatory Bowel Disease. *Plos One*. 2013; 8(4)
52. Seidelin JB, Bjerrum JT, Coskun M, Widjaya B, Vainer B, Nielsen OH. IL-33 is upregulated in colonocytes of ulcerative colitis. *Immunol Lett*. 2010; 128(1):80–85. [PubMed: 19913053]
53. Townsend MJ, Fallon PG, Matthews DJ, Jolin HE, McKenzie AN. T1/ST2-deficient mice demonstrate the importance of T1/ST2 in developing primary T helper cell type 2 responses. *J Exp Med*. 2000; 191(6):1069–1076. [PubMed: 10727469]
54. Guichard S, Chatelut E, Lochon I, Bugat R, Mahjoubi M, Canal P. Comparison of the pharmacokinetics and efficacy of irinotecan after administration by the intravenous versus intraperitoneal route in mice. *Cancer Chemother Pharmacol*. 1998; 42(2):165–170. [PubMed: 9654118]
55. Xiang D, Guo Y, Zhang J, Gao J, Lu H, Zhu S, et al. Interleukin-1 receptor antagonist attenuates cyclophosphamide-induced mucositis in a murine model. *Cancer Chemother Pharmacol*. 2011; 67(6):1445–1453. [PubMed: 20814790]
56. Souza DG, Guabiraba R, Pinho V, Bristow A, Poole S, Teixeira MM. IL-1-driven endogenous IL-10 production protects against the systemic and local acute inflammatory response following intestinal reperfusion injury. *J Immunol*. 2003; 170(9):4759–4766. [PubMed: 12707357]

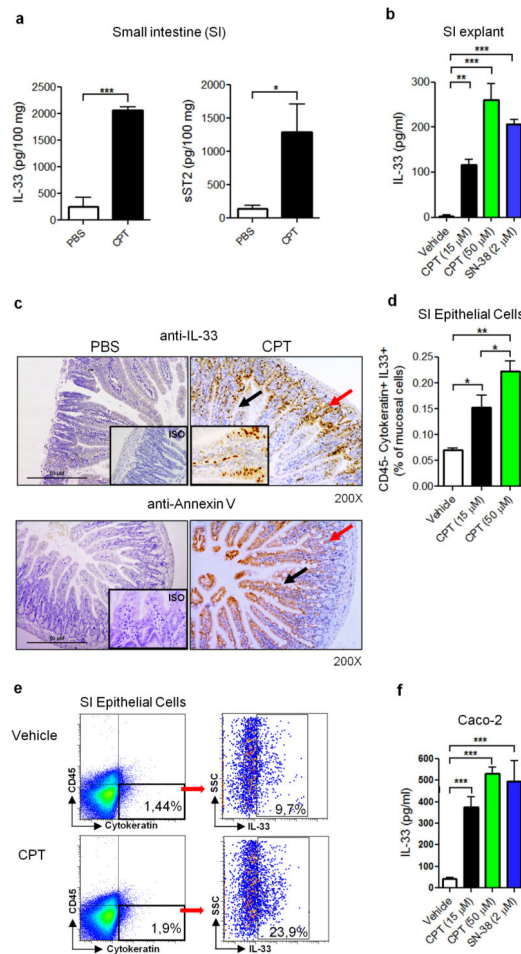


Figure 1.

IL-33 is produced in the small intestine in chemotherapy-induced mucositis. **(a)** IL-33 and sST2 concentrations in the small intestine (SI) of BALB/c mice after 4 daily injections of CPT-11 (60 mg/kg) or PBS were determined by ELISA. **(b)** IL-33 production in vitro by SI explants from BALB/c mice after 24 h incubation with CPT-11 or SN-38 measured by ELISA. **(c)** Representative IHC staining for IL-33 and Annexin V in the SI of PBS or CPT-11-treated mice at day 4. 200X magnification. Arrows indicate positive staining for IL-33 and Annexin V in the villi (black) and crypts (red). Inserts: ISO: 200X, CPT-11: 400X magnification. **(d)** The frequency of IL-33⁺CD45⁻cytokeratin⁺ epT cells from mice treated with CPT-11 or PBS (vehicle). **(e)** Representative FACS analysis showing the gating of IL-33⁺CD45⁻Cytokeratin⁺ epithelial cells (epT) isolated from WT mice treated with CPT-11 (50 μ M) for 6 h. **(f)** IL-33 concentration in the supernatant of Caco-2 cells cultured for 48 h with CPT-11 or SN-38 determined by ELISA. Results are representative of two independent experiments (n=3-5 mice per group). *P<0.05, **P<0.01, ***P<0.001

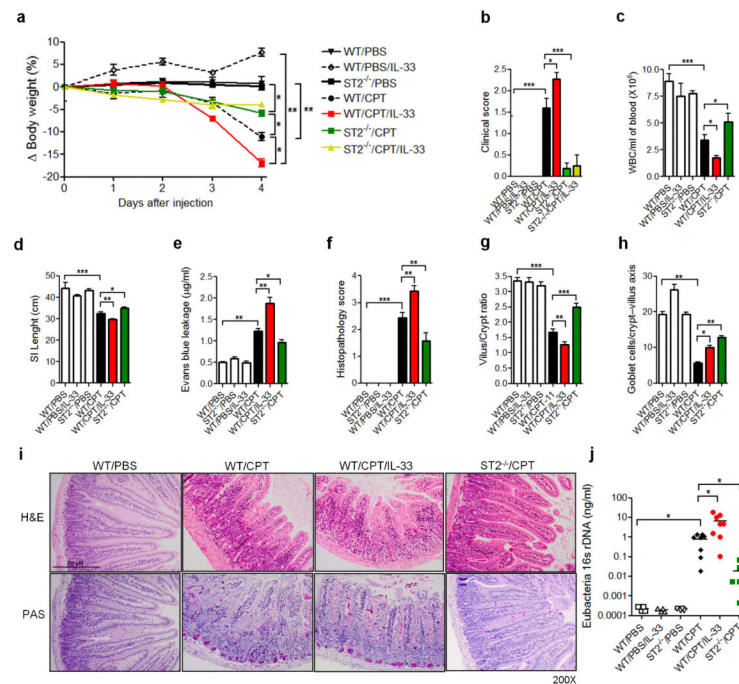
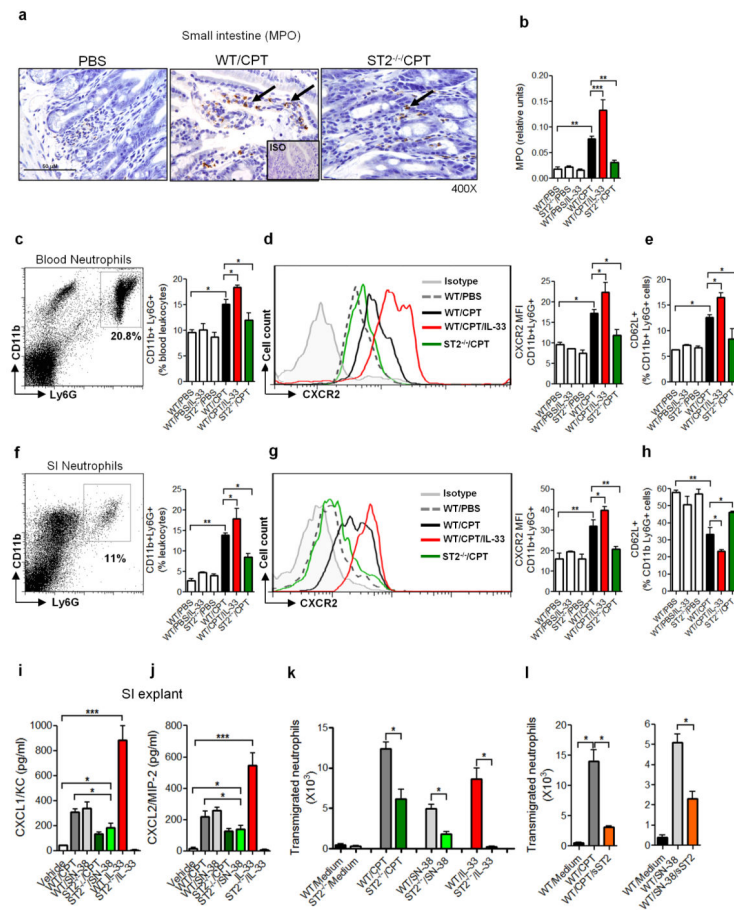
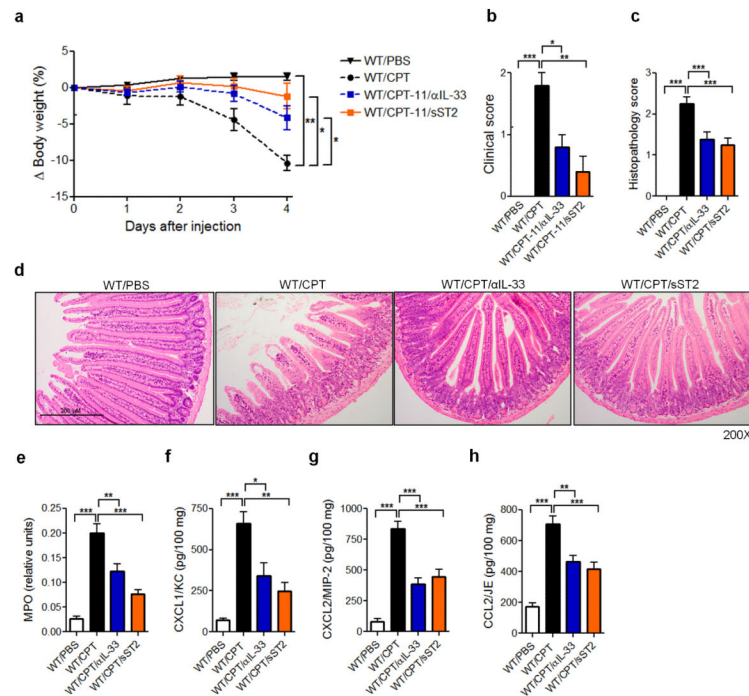


Figure 2.

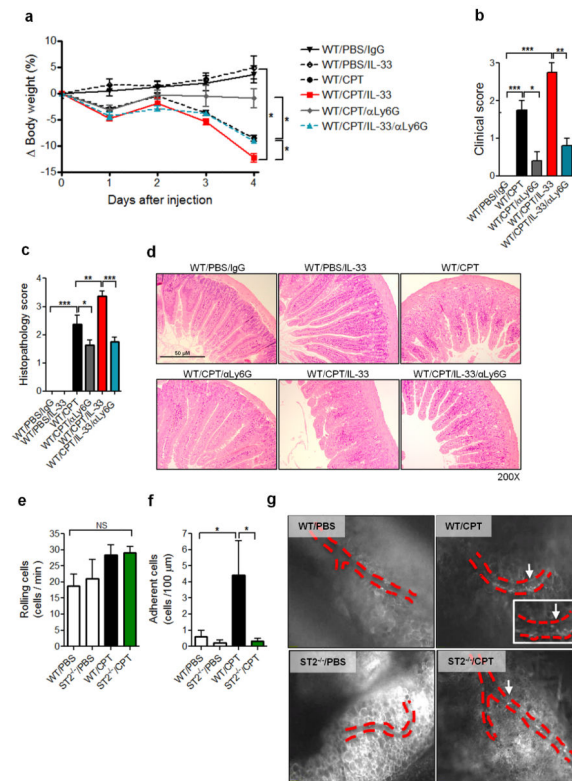
IL-33 is associated with the pathogenesis of chemotherapy-induced mucositis. WT and ST2^{-/-} mice were treated with CPT-11 or PBS with or without IL-33. **(a)** Body weight loss (%) was measured daily and **(b)** clinical score determined on day 4. **(c)** Whole blood cell (WBC) counts, **(d)** small intestine (SI) length, and **(e)** Evans blue leakage were also determined on day 5. **(f)** Histopathology score, **(g)** villus/crypt ratio, and **(h)** Goblet cell counts in the crypt-villus axis were also shown. **(i)** Representative histology of SI samples on day 5. **(j)** Expression of Eubacteria 16s rDNA in the blood was evaluated by qPCR on day 4. Data are pool of 2 experiments (n= 4-8 mice per group) and are representative of three independent experiments. *P<0.05, **P<0.01, ***P<0.001.

**Figure 3.**

Neutrophils play a key role in CPT-11/IL-33-induced intestinal mucositis. WT and ST2^{-/-} mice were treated with CPT-11 with or without IL-33. **(a)** Representative IHC staining for MPO in the SI on day 2. Arrows indicate positive staining for MPO of the villi. **(b)** Myeloperoxidase (MPO) activity in the SI on day 4. **(c)** Gating and representative percentage of blood CD11b⁺Ly6G⁺ neutrophils on day 2. **(d)** Representative Mean Fluorescence Intensity (MFI) of CXCR2 on blood CD11b⁺Ly6G⁺ neutrophils on day 2. **(e)** Percentage of CD62L⁺CD11b⁺Ly6G⁺ neutrophils in the blood on day 2. **(f)** Gating and representative percentage of CD11b⁺Ly6G⁺ neutrophils in the SI on day 4. **(g)** Representative MFI of CXCR2 on CD11b⁺Ly6G⁺ neutrophils in the SI on day 4. **(h)** Percentage of CD62L⁺CD11b⁺Ly6G⁺ cells in the SI on day 4. SI explants from WT and ST2^{-/-} mice were cultured for 24 h in the presence of CPT-11 (50 μM), SN-38 (2 μM) or IL-33 (10 ng/ml) and the concentrations of **(i)** CXCL1/KC and **(j)** CXCL2/MIP-2 determined by ELISA. **(k, l)** SI explants from WT or ST2^{-/-} mice were cultured with CPT-11, SN-38 or IL-33. Supernatants were collected after 24 h and placed in the lower chamber of transwell culture plates. WT Ly6G⁺ neutrophils were placed on the upper chamber. **(k)** The number of neutrophils in the lower chamber was determined 3 h later. **(l)** The number of trans-migrating neutrophils in the presence of sST2 (10 μg/ml) in the lower chamber was also shown. Results are representative of three independent experiments (n=5-6 mice per group). *P<0.05, **P<0.01, ***P<0.001.

**Figure 4.**

IL-33 blockade ameliorates CPT-11-induced intestinal mucositis. WT mice were treated with PBS or CPT-11 for 4 days and received anti-IL-33 (25 μ g/daily/s.c.) or sST2 (100 μ g/daily/s.c.). Data were analyzed on day 4. **(a)** Body weight loss; **(b)** clinical score; **(c)** histopathology score; **(d)** representative histology (H&E staining) of SI; **(e)** Myeloperoxidase (MPO) activity of SI. **(f)** CXCL1/KC, **(g)** CXCL2/MIP-2 and **(h)** CCL2/JE production in the SI determined by ELISA. Results are representative of two independent experiments (n=5 mice per group). *P<0.05, **P<0.01, ***P<0.001.

**Figure 5.**

Neutrophil depletion attenuates CPT-11-induced intestinal mucositis. BALB/c mice were treated with CPT-11 with or without IL-33. Some mice were injected s.c. with anti-Ly6G (100 μg) or control IgG on days 0 and 2. Data were analyzed on day 4. **(a)** Body weight loss; **(b)** Clinical score; **(c)** Histopathology score; **(d)** Representative histology of SI (H&E). Intra-vital microscopy was used to assess the rolling **(e)** and adhesion **(f)** of leukocytes on the mesenteric microvasculature on day 2 in WT and ST2^{-/-} mice. Data are pool of 2 experiments (n=8-10 mice per group). **(g)** Representative pictures of the mesenteric veins. Red dotted lines, blood vessels; white arrows, leukocytes attached to the vessels. Results are representative of two independent experiments (n=5 mice per group). *P<0.05, **P<0.01, ***P<0.001. Also see Supplementary Videos.

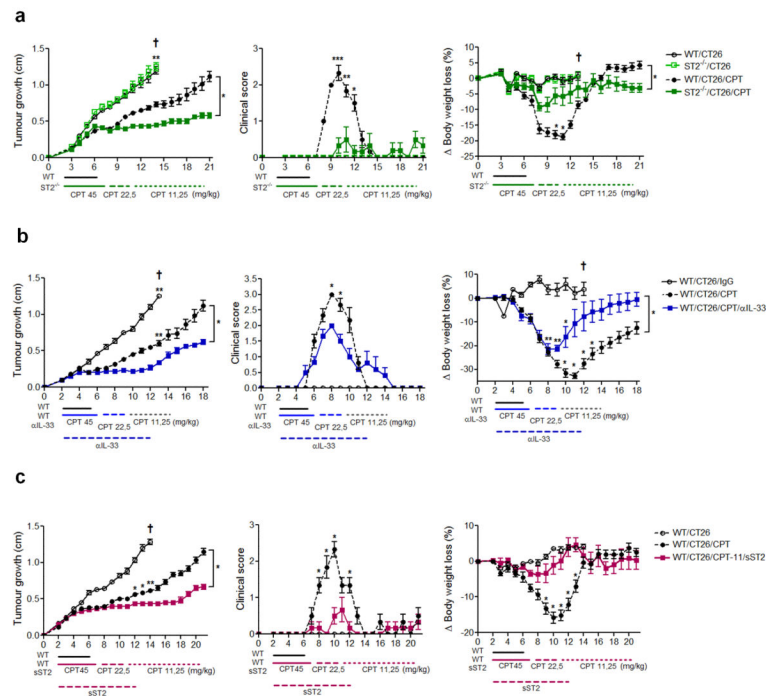


Figure 6.

IL-33 targeting attenuates intestinal mucositis and prolongs effective chemotherapy against tumour. WT and ST2^{-/-} mice were transplanted s.c. with CT26 colon carcinoma cells (1×10^6 cells). Some mice were treated with CPT-11 at indicated doses. Some WT mice were also injected daily s.c. (day 2-12) with anti-IL-33 (25 μ g) or sST2 (100 μ g). Tumour growth (mean diameter in cm), clinical score and body weight loss were recorded daily. (a) WT and ST2^{-/-} mice; (b) WT and anti-IL-33-treated mice; (c) WT and sST2-treated mice. Results are representative of two independent experiments (n=6 mice per group). Dark cross: mice were culled because of severity of disease. *P<0.05, **P<0.01, ***P<0.001. See Supplementary Figure S4 for pictures of tumour-bearing mice.

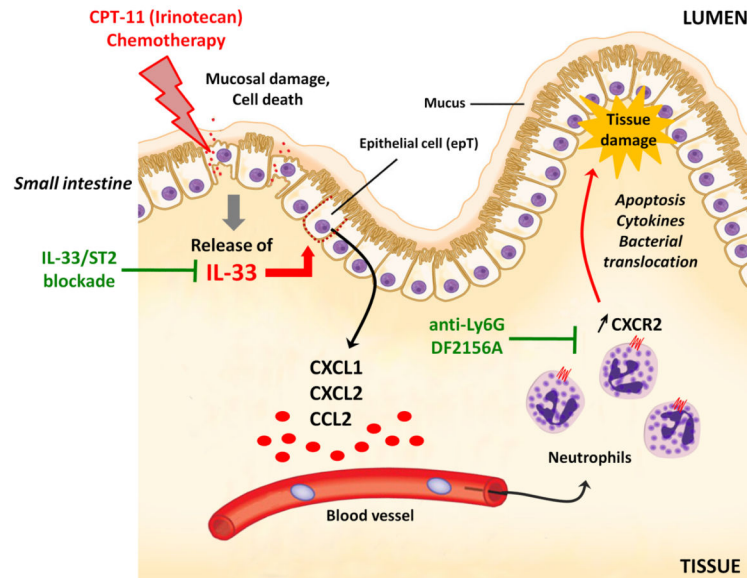


Figure 7.

Schematic representation of the mechanism of IL-33-mediated CPT-11-induced intestinal mucositis and potential therapeutic targets. CPT-11 damages the intestinal mucosa and releases IL-33, which enhances chemokines production from the epithelial cells and up-regulation of CXCR2 on neutrophils, thereby increasing the recruitment of neutrophils to the inflammatory sites, leading to further tissue damage and bacterial translocation. Blocking of IL-33 by anti-IL-33 antibody or sST2 attenuates CXC chemokine production and neutrophil activation/accumulation. Depletion of neutrophils or blocking CXCR2 would also attenuate tissue damage and disease outcome.